

Finite temperature Casimir effect of scalar field

Liang Chen(陈亮), Yu-Jing Wang(王钰婧), and Sheng-Yan Li(李生艳)
Citation: Chin. Phys. B, 2026, 35 (**7**): 074401. DOI: 10.1088/1674-1056/ae24ea
http://cpb.iphy.ac.cn; http://iopscience.iop.org/cpb

What follows is a list of articles you may be interested in

Finite element analysis of copper nanoparticles in Boger fluid: Effects of dynamic inter-particle spacing, nanolayer thermal conductivity, nanoparticles diameter, and thermal radiation over a stretching sheet

Qadeer Raza, Xiaodong Wang(王晓东), Tahir Mushtaq, Bagh Ali, and Nehad Ali Shah
Chin. Phys. B, 2025, 34 (**11**): 114402. DOI: 10.1088/1674-1056/addcbc

Cattaneo-Christov heat transfer model for tangent hyperbolic fluid with Thompson-Torian slip and melting effects

Anwar Saeed and Afrah Al-Bossly
Chin. Phys. B, 2025, 34 (**9**): 094404. DOI: 10.1088/1674-1056/add90a

Dual-band switchable mid-infrared emitter based on In_3SbTe_2 for gas detection application

Biyuan Wu(吴必园), Xiqiao Huang(黄希桥), and Xiaohu Wu(吴小虎)
Chin. Phys. B, 2025, 34 (**9**): 094403. DOI: 10.1088/1674-1056/ade59e

Experimental study on the regulation of radiative heat flux by coating SiC film

Haifeng Xia(閤海峰) and Huihui Sun(孙慧慧)
Chin. Phys. B, 2025, 34 (**5**): 054402. DOI: 10.1088/1674-1056/adbee0

Influence of substrate effect on near-field radiative modulator based on biaxial hyperbolic materials

Ruiyi Liu(刘睿一), Haotuo Liu(刘皓佗), Yang Hu(胡杨), Zheng Cui(崔峥), and Xiaohu Wu(吴小虎)
Chin. Phys. B, 2024, 33 (**4**): 044403. DOI: 10.1088/1674-1056/ad2a6c

---

Finite temperature Casimir effect of scalar field

Liang Chen(陈亮)[1,2,3,†], Yu-Jing Wang(王钰婧)[1,2], and Sheng-Yan Li(李生艳)[1,2]

[1] *School of Mathematics and Physics, North China Electric Power University, Beijing* 102206, *China*
[2] *Institute of Condensed Matter Physics, North China Electric Power University, Beijing* 102206, *China*
[3] *Hebei Key Laboratory of Physics and Energy Technology, North China Electric Power University, Baoding* 071003, *China*

(Received 3 September 2025; revised manuscript received 14 November 2025; accepted manuscript online 27 November 2025)

We derive analytical expressions for the Helmholtz free energy, Casimir force, and Casimir entropy in one- and three-dimensional scalar fields subject to Dirichlet boundary conditions at finite temperature. The problem of negative Casimir entropy is examined in these systems, as well as for a scalar field confined within a three-dimensional (3D) spherical cavity. Our analysis shows that this apparent paradox arises under different regularization schemes involving distinct counterterms. We advocate against introducing any counterterms for the thermal corrections to the Casimir effect and predict that the thermal-fluctuation-induced Casimir force becomes repulsive in the high-temperature limit, specifically when $aT/(\pi\hbar v) > 0.2419$ for the 3D scalar field.

Keywords: Casimir effect, Nernst theorem, finite-temperature quantum field theory

PACS: 44.40.+a, 62.25.–g, 65.40.gd, 11.10.–z

DOI: 10.1088/1674-1056/ae24ea **CSTR:** 32038.14.CPB.ae24ea

1. Introduction

The uncertainty principle in quantum mechanics dictates that a harmonic oscillator in any quantum state cannot be at absolute rest but must possess a finite zero-point energy. This fundamental principle extends naturally to quantum field theory, where a free-space quantum field can be viewed as a collection of harmonic oscillators labeled by distinct quantum numbers. Without regularization, the vacuum (ground state) energy of such a field diverges. Remarkably, altering the field's boundary conditions can yield measurable physical effects, most notably the Casimir effect.[1–5] Although the physical origin of the Casimir effect remains a subject of debate,[6] in this work we adopt the perspective of vacuum quantum fluctuations. Within this framework, electromagnetic vacuum fluctuations induce an attractive force between two parallel, neutral conducting plates. At zero temperature, this force is given by $-\pi^2 c\hbar/(240a^4)$, where a is the plate separation, $\hbar$ is the reduced Planck constant, and c is the speed of light in vacuum. This interaction becomes dominant at micron–nanometer scales, profoundly influencing the design, functionality, and performance of micro- and nano-electromechanical systems. Recent decades have witnessed substantial experimental advances across multiple frontiers of Casimir physics. These include repulsive Casimir forces,[7–9] the critical Casimir effect,[10–15] the dynamical Casimir effect,[16–19] experimental constraints on nonstandard forces,[20–25] and the Casimir–Lifshitz torque.[26] On the theoretical side, research has expanded in several directions. The Casimir effect has been shown to provide mechanisms for spontaneous compactification of extra spatial dimensions in theories beyond the Standard Model,[27] while experimental measurements can conversely constrain new theoretical proposals.[28] Repulsive Casimir interactions have been predicted in systems with specific geometries,[29] metamaterials,[30,31] topological matters,[32–35] or chiral media.[36] Furthermore, Casimir-like phenomena mediated by quantum excitations other than virtual photons have been explored, including those involving gravitational fields,[37] massless fermions,[38] neutrinos,[39] phonons,[40] and magnons,[41] significantly broadening the conceptual and applicative scope of the effect.

Despite these significant advances, a fundamental theoretical challenge persists in thermal Casimir physics, recently termed the "Casimir puzzle" and "Casimir conundrum" by Mostepanenko[42] and extensively investigated over the past two decades.[43–49] At its core lies an apparent incompatibility between the Drude model description of metals and dc conductivity in dielectrics, and the predictions of Lifshitz theory. This discrepancy manifests most strikingly in two ways: (i) systematic deviations between Drude-model predictions and experimental measurements, and (ii) the model's violation of the Nernst heat theorem due to its prediction of negative entropy.[50] In this work, we revisit the longstanding problem of the finite-temperature Casimir effect for both three-dimensional (3D) and one-dimensional (1D) scalar fields under Dirichlet boundary conditions. Our approach yields exact analytical expressions for the Helmholtz free energy, en-

†Corresponding author. E-mail: slchern@ncepu.edu.cn

© 2026 Chinese Physical Society and IOP Publishing Ltd. All rights, including for text and data mining, AI training, and similar technologies, are reserved.

abling a rigorous assessment of two commonly used regularization schemes: (i) subtraction of free-space thermal fluctuations, and (ii) removal of divergent high-temperature terms. Our exact results demonstrate that both types of counterterms are inherently inconsistent, as they lead to the emergence of negative Casimir entropy within these regularization prescriptions.

We begin by reviewing the finite-temperature Casimir effect for electromagnetic (EM) fields confined between ideal metal plates. A crucial aspect is that the transverse electric (TE) and transverse magnetic (TM) modes obey different boundary conditions: while TE modes satisfy Dirichlet conditions, TM modes require special treatment of the $k_z = 0$ component during field quantization. This leads to the Helmholtz free energy per unit area,

$$F_{\rm EM} = -\frac{\pi^2\hbar c}{360a^3} - \sum_{l=1}^{\infty}\left[\frac{lT^2}{\hbar ca}\mathrm{Li}_2\left(\mathrm{e}^{-l\pi\hbar c/aT}\right) + \frac{T^3}{\pi\hbar^2c^2}\mathrm{Li}_3\left(\mathrm{e}^{-l\pi\hbar c/aT}\right)\right] - \frac{\zeta(3)T^3}{2\pi\hbar^2c^2} + \frac{\pi^2aT^4}{45\hbar^3c^3}, \tag{1}$$

where T is the absolute temperature (with Boltzmann's constant $k_{\rm B} = 1$), and $\mathrm{Li}_n(z)$ and $\zeta(z)$ denote the polylogarithm and Riemann zeta functions respectively. The individual terms are explained as follows.

(i) The first term: the zero-temperature contribution from quantum fluctuations.

(ii) The summation over l: Contribution from thermal fluctuations of TE and TM modes, where l quantizes the wavevector $k_z = l\pi/a$.

(iii) The penultimate term: the $k_z = 0$ contribution of the TM mode.

(iv) The last term: the counterterm from free-space thermal radiation energy.

Notably, the $k_z = 0$ term exhibits unusual behavior: it neither depends on the plate separation a nor contributes to the Casimir force, influencing only the entropy. Further analysis yields the following asymptotic expressions for the Casimir entropy:

$$S\left(\frac{aT}{\hbar c}\to 0\right) \approx \frac{3\zeta(3)}{2\pi\hbar^2c^2}T^2 - \frac{4\pi^2}{45\hbar^3c^3}aT^3, \tag{2}$$

$$S\left(\frac{aT}{\hbar c}\to \infty\right) \approx \frac{\zeta(3)}{8\pi a^2}. \tag{3}$$

These results reveal the following two profound insights.

(i) Entropy saturation puzzle: Eq. (3) indicates that the Casimir entropy approaches a temperature-independent constant, a thermodynamically unexpected behavior, since entropy should grow indefinitely with the number of accessible quantum states at fixed a.

(ii) Salvation mechanism: The $k_z = 0$ TM mode term (the first term in Eq. (2)) exactly cancels the negative entropy that would otherwise arise from the counterterm (the second term in Eq. (2)). This observation raises our central question: What happens when such a stabilizing term is absent, as is the case for scalar fields subject to pure Dirichlet boundary conditions?

2. Three-dimensional scalar field

We first consider a massless scalar field in three spatial dimensions, governed by the wave equation (see Fig. 1 for illustration):

$$\left(\frac{\partial^2}{\partial t^2} - v^2\nabla^2\right)\phi(\boldsymbol{r},t) = 0, \tag{4}$$

where v denotes the phase velocity of the field.

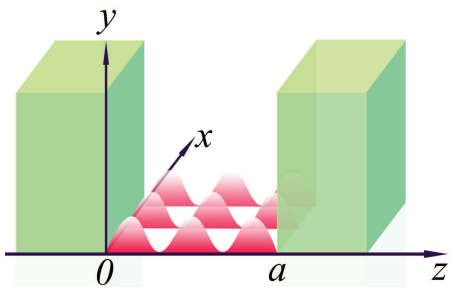


Fig. 1. Schematic diagram of the Casimir effect for a 3D scalar field confined to the region $0 < z < a$ with Dirichlet boundary conditions. The wave patterns within the region represent selected scalar field configurations.

Imposing Dirichlet boundary conditions at $z = 0$ and $z = a$,

$$\phi(\boldsymbol{r}_\parallel,0,t) = \phi(\boldsymbol{r}_\parallel,a,t) = 0, \tag{5}$$

and applying standard canonical quantization, we obtain the Helmholtz free energy per unit area (see Appendix A):

$$\frac{a^3}{v\hbar}F_{\rm 3D}^{\rm (I)} = -\frac{\pi^2}{1440} - \frac{\pi^2\theta^3}{2}\left(1 - \frac{\partial}{\partial s}\right) \times \sum_{l=1}^{\infty}\mathrm{Li}_3\left(\mathrm{e}^{-sl/\theta_3}\right)\Big|_{s=1}, \tag{6}$$

where $\theta_3 = aT/\pi\hbar v$ is the dimensionless temperature. The corresponding Casimir thermodynamic quantities, namely the Casimir force $P = -\partial F/\partial a$ and Casimir entropy $S = -\partial F/\partial T$, both per unit area, are then derived via direct differentiation:

$$\frac{a^4}{v\hbar}P_{\rm 3D}^{\rm (I)} = -\frac{\pi^2}{480} - \frac{\pi^2\theta_3}{2}\sum_{l=1}^{\infty}l^2\log\left(1 - \mathrm{e}^{-l/\theta_3}\right), \tag{7}$$

$$a^2S_{\rm 3D}^{\rm (I)} = \frac{3\pi}{2}\sum_{l=1}^{\infty}\left[\theta_3^2\,\mathrm{Li}_3(e^{-l/\theta_3}) + l\theta_3\,\mathrm{Li}_2(\mathrm{e}^{-l/\theta_3})\right.$$

$$-\frac{l^2}{3}\log(1-\mathrm{e}^{-l/\theta_3})\Big]. \tag{8}$$

Having derived the exact expressions, we now examine their asymptotic behavior in the low- and high-temperature regimes. In the low-temperature limit ($\theta_3 = aT/\pi\hbar v \ll 1$), the polylogarithm function

$$\mathrm{Li}_n(z) = \sum_{k=1}^{\infty}\frac{z^k}{k^n} \tag{9}$$

can be expanded to leading order, yielding simplified forms for the thermodynamic quantities. The Helmholtz free energy, Casimir force, and Casimir entropy reduce to

$$F_{3\mathrm{D}}^{(\mathrm{I})}(aT\to 0) \approx -\frac{\pi^2\hbar v}{1440a^3}\left[1+720\left(\frac{aT}{\pi\hbar v}\right)^2\mathrm{e}^{-\pi\hbar v/aT}\right], \tag{10}$$

$$P_{3\mathrm{D}}^{(\mathrm{I})}(aT\to 0) \approx -\frac{\pi^2\hbar v}{480a^4}\left(1-240\frac{aT}{\pi\hbar v}\mathrm{e}^{-\pi\hbar v/aT}\right), \tag{11}$$

$$S_{3\mathrm{D}}^{(\mathrm{I})}(aT\to 0) \approx \frac{\pi}{2a^2}\left(1+\frac{2aT}{\pi\hbar v}\right)\mathrm{e}^{-\pi\hbar v/aT}. \tag{12}$$

In the opposite high-temperature limit ($\theta_3 = aT/\pi\hbar v \gg 1$), the Casimir entropy asymptotically approaches

$$S_{3\mathrm{D}}^{(\mathrm{I})}(aT\gg\pi\hbar v) \approx \frac{\zeta(3)}{16\pi a^2} - \frac{3\zeta(3)}{4\pi\hbar^2v^2}T^2 + \frac{2\pi^2}{45\hbar^3v^3}aT^3. \tag{13}$$

Correspondingly, the Helmholtz free energy is approximated as follows:

$$F_{3\mathrm{D}}^{(\mathrm{I})}(aT\gg\pi\hbar v) \approx -\frac{\pi^2\hbar v}{1440a^3} - \frac{\zeta(3)}{16\pi a^2}T + \frac{\zeta(3)}{4\pi\hbar^2v^2}T^3 - \frac{\pi^2 a}{90\hbar^3v^3}T^4, \tag{14}$$

from which the temperature-dependent Casimir force is obtained as

$$P_{3\mathrm{D}}^{(\mathrm{I})}(aT\gg\pi\hbar v) \approx -\frac{\pi^2\hbar v}{480a^4} - \frac{\zeta(3)}{8\pi a^3} + \frac{\pi^2}{90\hbar^3v^3}T^4. \tag{15}$$

The high-temperature asymptotic expressions (Eqs. (13)–(15)) reveal a remarkable feature: when thermal fluctuations dominate ($aT \gg \pi\hbar v$), the Casimir force becomes repulsive and assumes a distance-independent form,

$$P_{3\mathrm{D}}^{(\mathrm{I})} \approx \frac{\pi^2}{90\hbar^3v^3}T^4. \tag{16}$$

Figure 2 shows the full temperature dependence of (a) the Helmholtz free energy, (b) the Casimir force, and (c) the Casimir entropy, together with their low- and high-temperature approximations. The curves exhibit excellent agreement between these approximations and the exact results in their respective temperature regimes. Notably, the transition between attractive and repulsive force regimes can be estimated analytically from the low-temperature expansion. This yields the critical ratio $aT/\pi\hbar v \approx W(240) = 0.2454$, where W denotes the Lambert W function. The analytical estimate agrees closely with the numerically determined transition point at 0.2419, with a relative error below 1.5%.

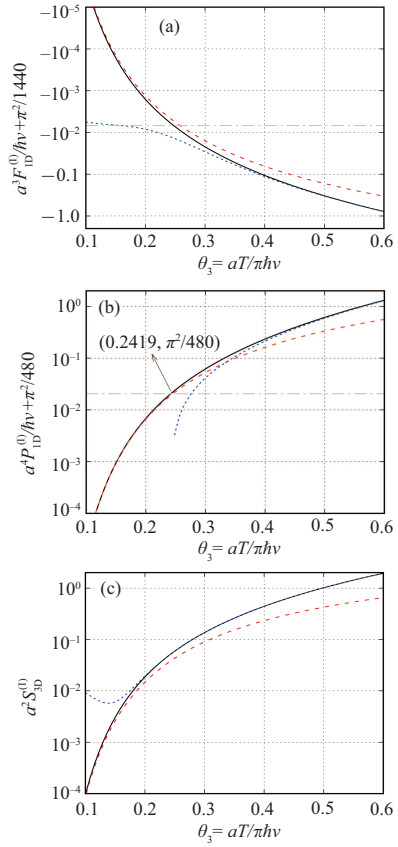


Fig. 2. Helmholtz free energy (a), Casimir force (b), and Casimir entropy (c) as functions of the dimensionless temperature $\theta_3 = aT/\pi\hbar v$ for the 3D scalar field with Dirichlet boundary conditions. Solid black lines represent the exact results, dashed red the low-temperature approximations, and dotted blue lines the high-temperature approximations. For clarity, the Helmholtz free energy, Casimir force, and Casimir entropy are scaled by $a^3/\hbar v$, $a^4/\hbar v$, and a^2, respectively.

We now examine how different regularization prescriptions affect the Casimir entropy. The aT^4 term in Eq. (14) corresponds precisely to the thermal correction from the free-space Helmholtz energy density within the cavity $0 < z < a$:

$$a\mathcal{F}_{\mathrm{free}} = a\int\frac{\mathrm{d}\boldsymbol{k}}{(2\pi)^3}\left[\frac{1}{\beta}\log\left(1-\mathrm{e}^{-\beta v\hbar k}\right)\right] = -\frac{\pi^2aT^4}{90v^3\hbar^3}. \tag{17}$$

A common regularization approach introduces a counterterm to subtract this free-space contribution, redefining the Helmholtz free energy as:

$$F_{3\mathrm{D}}^{(\mathrm{II})} = F_{3\mathrm{D}}^{(\mathrm{I})} - a\mathcal{F}_{\mathrm{free}}. \tag{18}$$

Although this prescription eliminates the distance-independent repulsive force in the high-temperature limit

$(aT/\pi\hbar v \gg 1)$, it leads to an unphysical consequence: the final term in Eq. (13) is also removed, yielding

$$S_{3D}^{(II)}(aT \gg \pi\hbar v) \approx \frac{\zeta(3)}{16\pi a^2} - \frac{3\zeta(3)}{4\pi\hbar^2 v^2} T^2 < 0, \tag{19}$$

which results in negative Casimir entropy across all temperatures, not only in the high-temperature regime. The authors in Ref. [51] proposed a modified prescription that additionally subtracts the T^3 and T^2 terms

$$F_{3D}^{(III)} = F_{3D}^{(I)} - a\mathcal{F}_{\text{free}} - \frac{\zeta(3)}{4\pi\hbar^2 v^2} T^3. \tag{20}$$

This alternative prescription yields positive entropy that saturates at $\zeta(3)/16\pi a^2$ in the high-temperature limit, resembling the behavior in the EM field case. However, a fundamental question persists: Is the subtraction of T^4, T^3, and T^2 terms universally valid? To address this, we analyze the scalar field in a 3D spherical geometry.

3. Scalar field in a 3D sphere

We consider a massless scalar field confined within a spherical cavity of radius a under Dirichlet boundary conditions. The quantized field takes the form

$$\hat{\phi}(\boldsymbol{r},t) = \sum_{l,s} \left[\hat{a}_{l,s}\, \mathrm{e}^{-\mathrm{i}\omega_{l,s}t} \psi_{l,s}(\boldsymbol{r}) + \hat{a}_{l,s}^{\dagger}\, \mathrm{e}^{\mathrm{i}\omega_{l,s}t} \psi_{l,s}^{*}(\boldsymbol{r}) \right], \tag{21}$$

where the eigenmodes

$$\psi_{l,s}(\boldsymbol{r}) = \mathrm{j}_l(ka)\mathrm{Y}_{l,m}(\vartheta,\varphi)/\sqrt{N_{l,s}}$$

satisfy the eigenvalue equation

$$-\frac{v^2}{r^2}\left(\frac{\partial}{\partial r} r^2 \frac{\partial}{\partial r} - \frac{L^2}{\hbar^2}\right) \psi_{l,s}(\boldsymbol{r}) = v^2 k_{l,s}^2 \psi_{l,s}(\boldsymbol{r}). \tag{22}$$

Here $\mathrm{Y}_{l,m}$ are spherical harmonics with angular momentum quantum number l (satisfying $L^2\mathrm{Y}_{l,m} = l(l+1)\mathrm{Y}_{l,m}$), and the index s labels the zeros of the spherical Bessel function,

$$\mathrm{j}_l(k_{l,s}a) = 0. \tag{23}$$

The corresponding eigenfrequencies are given by $\omega_{l,s} = vk_{l,s}$.

The Hamiltonian diagonalizes as

$$\hat{H} = \sum_{l,s} \frac{\hbar v k_{l,s}}{2} \left(\hat{a}_{l,s}\hat{a}_{l,s}^{\dagger} + \hat{a}_{l,s}^{\dagger}\hat{a}_{l,s} \right), \tag{24}$$

leading to the Helmholtz free energy

$$F_{\text{sphere}}^{(I)} = -T \log \left[\prod_{l,s} \sum_{n=0}^{\infty} \mathrm{e}^{-(n+1/2)\hbar v k_{l,s}} \right], \tag{25}$$

which naturally separates into zero-temperature quantum fluctuations and thermal contributions

$$F_{\text{sphere}}^{(I)} = F_{\text{sphere}}^{(I)}(T=0) + \delta F_{\text{sphere}}^{(I)}. \tag{26}$$

The zero-temperature contribution from quantum fluctuations takes the standard form

$$F_{\text{sphere}}^{(I)}(T=0) = \frac{\hbar v}{2} \sum_{l=0}^{\infty} \sum_{s=1}^{\infty} (2l+1) k_{l,s}. \tag{27}$$

As shown in previous studies,[52–55] the Casimir energy at zero temperature, after proper regularization, is given by

$$F_{\text{sphere}}^{(I)}(T=0) = C\frac{\hbar v}{2a}, \tag{28}$$

where the dimensionless coefficient $C = 0.00562$.

Our primary interest lies in the thermal fluctuation contribution,

$$\delta F_{\text{sphere}}^{(I)} = T \sum_{l=0}^{\infty} \sum_{s=1}^{\infty} (2l+1) \log(1 - \mathrm{e}^{-\hbar v k_{l,s}/T}). \tag{29}$$

Introducing the dimensionless temperature, $\theta_3 = aT/\pi\hbar v$, the Casimir self-entropy $S = -\partial F/\partial T$ becomes

$$\begin{aligned} S_{\text{sphere}}^{(I)} = &- \sum_{l=0}^{\infty} \sum_{s=1}^{\infty} (2l+1) \log(1 - \mathrm{e}^{-\rho_{l,s}/\pi\theta_3}) \\ &+ \sum_{l=0}^{\infty} \sum_{s=1}^{\infty} (2l+1) \frac{\rho_{l,s}}{\pi\theta_3} \frac{1}{\mathrm{e}^{\rho_{l,s}/\pi\theta_3} - 1}, \end{aligned} \tag{30}$$

where $\rho_{l,s}$ are the zeros of the spherical Bessel function, and the factor $2l+1$ accounts for the degeneracy in the magnetic quantum number.

Numerical evaluation of the Casimir self-entropy via Eq. (30) (see https://doi.org/10.57760/sciencedb.j00113.00260) includes all eigenmodes with angular and radial quantum numbers up to $l = s = 1000$, corresponding to 10^6 distinct eigenenergies. In the high-temperature regime ($\theta_3 = aT/\pi\hbar v \gg 1$), the entropy follows the polynomial expansion:

$$S_{\text{sphere}}^{(I)} = c_0 + c_1\theta_3 + c_2\theta_3^2 + c_3\theta_3^3. \tag{31}$$

Based on the numerical results, we obtain the fitted coefficients $c_0 = -0.14178$, $c_1 = 2.18011$, $c_2 = -17.7946$, and $c_3 = 56.9712$ over the range $1 \le \theta_3 \le 14$. These values are consistent with the analytical results reported in Ref. [56]. Details of the computational subroutines used to evaluate the Casimir self-entropy, along with numerical results for additional parameter sets $(l,s) = (800,500)$, $(800,1000)$, and $(1000,500)$, are provided in Science Data Bank. The numerical convergence of these results has been verified. Notably, the cubic term exactly matches the blackbody radiation entropy for a free space volume $V = 4\pi a^3/3$

$$\frac{4\pi a^3}{3}\mathcal{S}_{\text{free}} = \frac{8\pi^6}{135}\theta_3^3 = 56.9712\theta_3^3, \tag{32}$$

where $\mathcal{S}_{\text{free}} = -\partial\mathcal{F}_{\text{free}}/\partial T$ is derived from the Helmholtz free energy density, $\mathcal{F}_{\text{free}}$. This high-precision agreement validates our numerical approach. Figure 3 shows the high-temperature

behavior of the Casimir self-entropy along with the polynomial fit from Eq. (31), revealing a fundamental regularization dilemma:

(i) Subtracting only the blackbody term $c_3\theta_3^3$ still yields negative entropy due to $c_2 < 0$.

(ii) Removing all divergent terms ($c_1\theta_3$ through $c_3\theta_3^3$) again results in negative entropy, as $c_0 < 0$.

(iii) An ad hoc prescription that retains only the $c_1\theta_3$ term maintains positivity but lacks physical justification.

This ambiguity highlights the need for universally consistent regularization standards, motivating our subsequent analysis of the 1D scalar field case.

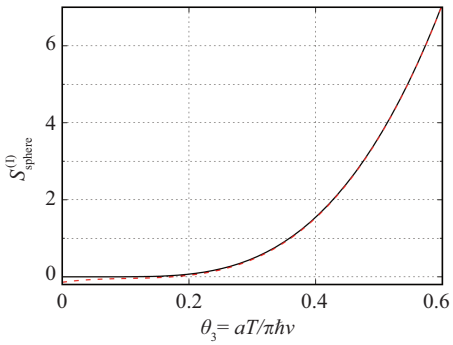


Fig. 3. The Casimir self-entropy of a scalar field in a 3D spherical cavity as a function of the dimensionless temperature scaled by the radius. The solid line represents the full numerical result, while the dashed line shows the high-temperature approximation from Eq. (31).

4. One-dimensional scalar field

We now consider a massless scalar field in one spatial dimension (as shown in Fig. 4), governed by the following wave equation

$$\left(\frac{\partial^2}{\partial t^2} - v^2\frac{\partial^2}{\partial x^2}\right)\phi(x,t) = 0, \tag{33}$$

where v is the phase velocity.

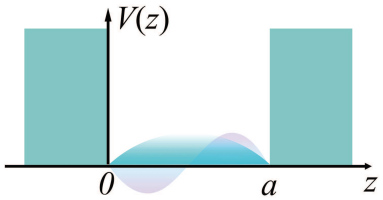


Fig. 4. The schematic diagram of a 1D scalar field confined to the interval $[0,a]$ under Dirichlet boundary conditions. Quantum fluctuations of the field induce a Casimir interaction between the boundaries. The waveforms shown between the boundaries represent two representative field modes with eigenenergies $E_n(1)$ and $E_n(2)$, respectively.

Under the Dirichlet boundary conditions $\phi(0,t) = \phi(a,t) = 0$, the Helmholtz free energy takes a particularly compact form (see Appendix A),

$$F^{(\mathrm{I})}_{1\mathrm{D}} = T\log\left[\eta\left(\frac{\mathrm{i}v\hbar}{2aT}\right)\right], \tag{34}$$

where $\eta(z)$ denotes the Dedekind η function defined on the upper half complex plane. The Casimir force $P = -\partial F/\partial a$ and entropy $S = -\partial F/\partial T$ follow by direct differentiation

$$P^{(\mathrm{I})}_{1\mathrm{D}} = \frac{\mathrm{i}v\hbar}{2a^2}\frac{\eta'(\mathrm{i}v\hbar/2aT)}{\eta(\mathrm{i}v\hbar/2aT)}, \tag{35}$$

$$S^{(\mathrm{I})}_{1\mathrm{D}} = -\log\left[\eta\left(\frac{\mathrm{i}v\hbar}{2aT}\right)\right] + \frac{\mathrm{i}v\hbar}{2aT}\frac{\eta'(\mathrm{i}v\hbar/2aT)}{\eta(\mathrm{i}v\hbar/2aT)}. \tag{36}$$

Introducing the dimensionless temperature $\theta_1 = aT/v\hbar$, we obtain the simplified expressions

$$\frac{a}{v\hbar}F^{(\mathrm{I})}_{1\mathrm{D}} = \theta_1\log\left[\eta\left(\frac{\mathrm{i}}{2\theta_1}\right)\right], \tag{37}$$

$$\frac{a^2}{v\hbar}P^{(\mathrm{I})}_{1\mathrm{D}} = \frac{\mathrm{i}}{2}\frac{\eta'(\mathrm{i}/2\theta_1)}{\eta(\mathrm{i}/2\theta_1)}, \tag{38}$$

$$S^{(\mathrm{I})}_{1\mathrm{D}} = -\log\left[\eta\left(\frac{\mathrm{i}}{2\theta_1}\right)\right] + \frac{\mathrm{i}}{2\theta_1}\frac{\eta'(\mathrm{i}/2\theta_1)}{\eta(i/2\theta_1)}. \tag{39}$$

Having established the exact solutions for the 1D scalar field in Eqs. (34)–(36), we now examine their asymptotic limits to reveal the underlying thermodynamic behavior. In the low-temperature regime ($\theta_1 = aT/v\hbar \ll 1$), the Dedekind η function admits the approximation,[57,58]

$$\eta(z) = A\frac{q^{1/24}}{\sqrt{1-q}}\exp\left[-\frac{\pi^2}{6(1-q)}\right], \quad (q = \mathrm{e}^{2\mathrm{i}\pi z}), \tag{40}$$

where the coefficient A is determined by requiring $S(T \to 0) = 0$, yielding $A = \mathrm{e}^{\pi^2/6}$. This leads to the following low-temperature approximations

$$\frac{a}{v\hbar}F^{(\mathrm{I})}_{1\mathrm{D}} = -\frac{\pi}{24} - \frac{\theta_1}{2}\left(\frac{\pi^2}{3} - 1\right)\mathrm{e}^{-\pi/\theta_1}, \tag{41}$$

$$\frac{a^2}{v\hbar}P^{(\mathrm{I})}_{1\mathrm{D}} = -\frac{\pi}{24} + \frac{\pi}{2}\left(\frac{\pi^2}{3} - 1\right)\mathrm{e}^{-\pi/\theta_1}, \tag{42}$$

$$S^{(\mathrm{I})}_{1\mathrm{D}} = \frac{\pi}{2}\left(\frac{\pi^2}{3} - 1\right)\left(\frac{\pi}{\theta_1} + 1\right)\mathrm{e}^{-\pi/\theta_1}. \tag{43}$$

In the high-temperature regime (*i.e.*, $\theta_1 = aT/v\hbar \gg 1$), we apply the modular transformation property of the Dedekind η function,

$$\eta(z) = \sqrt{\frac{\mathrm{i}}{z}}\eta\left(-\frac{1}{z}\right), \tag{44}$$

to the Helmholtz free energy in Eq. (34), yielding the equivalent expression:

$$F^{(\mathrm{I})}_{1\mathrm{D}} = T\log\left[\sqrt{2\theta_1}\eta(2\mathrm{i}\theta_1)\right]. \tag{45}$$

Substituting the asymptotic form of the η function, Eq. (40), into this expression gives the high-temperature approximations

$$\frac{a}{v\hbar}F^{(\mathrm{I})}_{1\mathrm{D}} = \frac{\log(2\theta_1)}{2}\theta_1 - \frac{\pi}{6}\theta^2 - \frac{1}{2}\left(\frac{\pi^2}{3} - 1\right)\mathrm{e}^{-4\pi\theta_1}, \tag{46}$$

$$\frac{a^2}{v\hbar}P^{(\mathrm{I})}_{1\mathrm{D}} = -\frac{\theta_1}{2} + \frac{\pi}{6}\theta^2 - 2\pi\left(\frac{\pi^2}{3} - 1\right)\theta_1^2\,\mathrm{e}^{-4\pi\theta_1}, \tag{47}$$

$$S_{1D}^{(I)} = -\frac{1+\log(2\theta_1)}{2} + \frac{\pi}{3}\theta_1 - \frac{1}{2}\left(\frac{\pi^2}{3}-1\right)(4\pi\theta_1 - 1)\,e^{-4\pi\theta_1}. \quad (48)$$

Numerical evaluation confirms excellent agreement between these asymptotic approximations and the exact solutions (as shown in Fig. 5). Notably, the Casimir entropy remains positive at all temperatures when no counterterms are introduced.

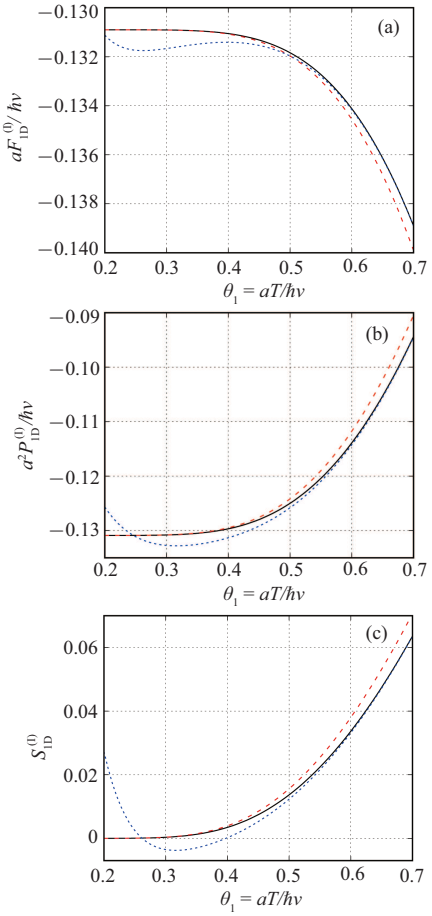


Fig. 5. Helmholtz free energy (a), Casimir force (b), and Casimir entropy (c) as functions of the dimensionless temperature $\theta_1 = aT/\hbar v$ for the 1D scalar field with Dirichlet boundary conditions. Solid black lines represent exact results, dashed red lines show the low-temperature approximation, and dotted blue lines indicate high-temperature approximations. For dimensionless representation, the Helmholtz free energy and Casimir force are scaled by $a/\hbar v$ and $a^2/\hbar v$, respectively.

We now examine how different regularization prescriptions affect the Casimir entropy. The thermal fluctuation contribution to the free energy density in unbounded space is given by

$$a\mathcal{F}_{\text{free}} = aT\int_{-\infty}^{\infty}\frac{dk}{2\pi}\log\left(1-e^{-v\hbar k/T}\right) = -\frac{\pi}{6}\frac{aT^2}{v\hbar}, \quad (49)$$

Adopting this term as a counterterm removes the leading divergence in Eq. (46) at high temperatures:

$$F_{1D}^{(II)} = F_{1D}^{(I)} - a\mathcal{F}_{\text{free}} = T\log\left[\eta\left(\frac{iv\hbar}{2aT}\right)\right] + \frac{\pi}{6}\frac{aT^2}{v\hbar}. \quad (50)$$

This modification eliminates the dominant positive Casimir entropy contribution, yielding

$$S_{1D}^{(II)}(\theta_1 \gg 1) = -\frac{\partial F_{1D}^{(II)}}{\partial T} \approx -\frac{1+\log(2\theta_1)}{2} - \frac{1}{2}\left(\frac{\pi^2}{3}-1\right)(4\pi\theta_1 - 1)\,e^{-4\pi\theta_1}. \quad (51)$$

The Casimir entropy becomes negative to leading order in $e^{-4\pi\theta_1}$ and remains negative at all temperatures when evaluated via Eq. (51). We have systematically tested alternative regularization prescriptions (see Table 1 and Fig. 6 for details).

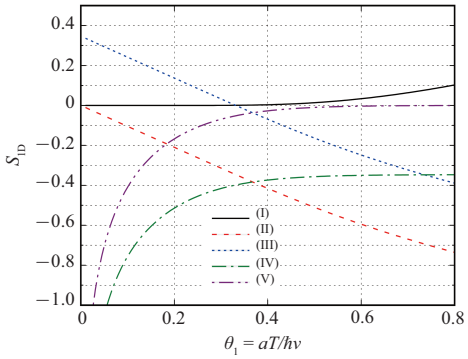


Fig. 6. Casimir entropy under different counterterm prescriptions for the 1D scalar field with Dirichlet boundary condition. Details of the counterterms are provided in Table 1. The solid black line corresponds to the unmodified result (prescription I) without counterterms.

All prescriptions result in negative Casimir entropy in some or all temperature ranges. This underscores a persistent challenge: using the free-space thermal fluctuation as a counterterm necessarily introduces negative Casimir entropy. For the one-dimensional scalar field with Dirichlet boundary conditions, no physically justified counterterm prescription avoids this outcome.

Table 1. Summarizing different regularization prescriptions.

Prescription	Counterterm in Helmholtz free energy $(a/\hbar v)/(F_{1D}^{(\text{ind.})} - F_{1D}^{(I)})$	Modification of Casimir entropy $(S_{1D}^{(\text{ind.})} - S_{1D}^{(I)})$
(I)	–	–
(II)	$(\pi/6)\theta_1^2$	$-(\pi/3)\theta_1$
(III)	$(\pi/6)\theta_1^2 - (1/2)\log(2)\theta_1$	$-(\pi/3)\theta_1 + (1/2)\log(2)$
(IV)	$(\pi/6)\theta_1^2 - (1/2)\theta_1\log(\theta_1)$	$-(\pi/3)\theta_1 + (1/2)[\log(\theta_1)+1]$
(V)	$(\pi/6)\theta_1^2 - (1/2)\theta_1\log(2\theta_1)$	$-(\pi/3)\theta_1 + (1/2)[\log(2\theta_1)+1]$

5. Summary

We have systematically investigated the finite-temperature Casimir effect for scalar fields in one and three spatial dimensions. For the 3D scalar field confined between parallel plates ($0 < z < a$) with Dirichlet boundary conditions, our analysis reveals that: (i) Using only the free-space thermal radiation energy as a counterterm leads to negative Casimir entropy. (ii) Including additional T^3 and T^2 terms in the counterterm prescription restores positive entropy, with the high-temperature limit approaching $\zeta(3)/(16\pi a^2)$. (iii) For the spherical geometry, high-precision numerical calculations show that even this extended prescription fails, yielding a negative high-temperature entropy limit (~ -0.12).

In the 1D case with exact solutions, all four tested counterterm schemes (listed in Table 1) produce negative entropy in certain temperature regimes. These findings extend previous studies of negative entropy,[59–62] demonstrating that even for simple Dirichlet boundary conditions with exact solutions, conventional counterterm approaches face fundamental challenges.

Our results raise important questions about standard regularization prescriptions: (I) While mathematically convenient for removing divergences, counterterms may lack physical justification when finite results can be obtained without them. (II) The persistent negative entropy problem suggests deeper issues in thermal Casimir physics that warrant re-examination of standard approaches, including the Lifshitz formula and quantum field theoretic treatments.

Notably, within our proposed framework (prescription I), the theory predicts a sign reversal of the Casimir force for a dimensionless temperature $\theta_3 = aT/\pi c\hbar \gtrsim 0.2419$. Under ambient conditions ($T = 300$ K) and in an ideal scenario of perfect Dirichlet boundaries with $v = c$, this translates to a separation $a \gtrsim 5.8$ μm, a scale broadly comparable to those accessed in modern Casimir experiments.[63] This theoretically predicted repulsive regime, which arises when thermal fluctuations dominate over vacuum contributions, highlights the critical role of regularization in determining the force's sign and offers a conceptually testable implication of our approach.

Acknowledgment

Project supported by the National Natural Science Foundation of China (Grant No. 12174101) and the Fundamental Research Funds for the Central Universities (Grant No. 2022MS051).

Appendix A

Here we present a detailed derivation of the Helmholtz free energy for both 3D and 1D massless scalar fields under Dirichlet boundary conditions, as referenced in the main text.

A1 Three-dimensional scalar field

Via canonical quantization, energy eigenvalues of 3D massless scalar field, governed by Eq. (4) in the main text and subject to Dirichlet boundary conditions at $z = 0$ and $z = a$, are given by

$$E_n(\boldsymbol{k}_\parallel, l) = (n + 1/2)\hbar v\sqrt{k_\parallel^2 + (l\pi/a)^2}, \tag{A1}$$

where $\boldsymbol{k}_\parallel = (k_x, k_y)$ is the in-plane wavevector parallel to the boundaries. Here, the integer $l = 1, 2, \ldots$ labels the discrete transverse modes along the confined z-direction, and $n = 0, 1, 2, \ldots$ denotes the particle number occupation. The corresponding partition function reads

$$Z_{3\mathrm{D}} = \prod_{l,\boldsymbol{k}_\parallel} \sum_{n=0}^{\infty} \mathrm{e}^{-E_n(\boldsymbol{k}_\parallel, l)/T}. \tag{A2}$$

Using the standard thermodynamic relation $F = -T\log(Z)$, the Helmholtz free energy per unit area becomes

$$\begin{aligned} F_{3\mathrm{D}}^{(\mathrm{I})} = &\sum_{l=1}^{\infty}\int_0^{\infty}\frac{k_\parallel \mathrm{d}k_\parallel}{2\pi}\frac{1}{2}v\hbar\sqrt{k_\parallel^2 + \left(\frac{l\pi}{a}\right)^2} \\ &+ T\sum_{l=1}^{\infty}\int_0^{\infty}\frac{k_\parallel \mathrm{d}k_\parallel}{2\pi}\log\left[1 - \mathrm{e}^{-\beta v\hbar\sqrt{k_\parallel^2 + (l\pi/a)^2}}\right]. \end{aligned} \tag{A3}$$

To evaluate this expression, the first term is regularized via the Riemann zeta-function technique, while in the second term we apply the substitution, $u = \sqrt{k_\parallel^2 + (l\pi/a)^2}$, leading to the following expression

$$\begin{aligned} F_{3\mathrm{D}}^{(\mathrm{I})} = &-\frac{\pi^2 v\hbar}{1440a^3} \\ &+ \frac{T}{4\pi}\sum_{l=1}^{\infty}\int_{\left(\frac{l\pi}{a}\right)^2}^{\infty}\log\left(1 - \mathrm{e}^{-v\hbar/T\sqrt{u}}\right)\mathrm{d}u. \end{aligned} \tag{A4}$$

The integral in the second term of Eq. (A4) can be rewritten in terms of the polylogarithm function $\mathrm{Li}_n(z)$ as

$$\begin{aligned} \frac{a^3}{v\hbar}F_{3\mathrm{D}}^{(\mathrm{I})} = &-\frac{\pi^2}{1440} - \frac{\pi^2\theta^3}{2}\left(1 - \frac{\partial}{\partial s}\right) \\ &\times \sum_{l=1}^{\infty}\mathrm{Li}_3\left(\mathrm{e}^{-sl/\theta_3}\right)\Big|_{s=1}. \end{aligned} \tag{A5}$$

A2 One-dimensional scalar field

For 1D massless scalar field described by Eq. (33) in the main text, field quantization yields discrete eigenenergies

$$E_n(l) = \left(n + \frac{1}{2}\right)\hbar v\frac{l\pi}{a}, \tag{A6}$$

where $n = 0, 1, 2, \ldots$ is the particle number index and $l = 1, 2, 3, \ldots$ quantizes the wavevector as $k = l\pi/a$. The finite-temperature partition function is then

$$Z = \prod_{l=1}^{\infty}\sum_{n=0}^{\infty}\mathrm{e}^{-E_n(l)/T} = \prod_{l=1}^{\infty}\frac{\exp(-l\pi v\hbar/2aT)}{1 - \exp(-l\pi v\hbar/aT)}, \tag{A7}$$

from which the Helmholtz free energy $F = -T\log(Z)$ becomes

$$F_{1\mathrm{D}}^{(\mathrm{I})} = \sum_{l=1}^{\infty}\left\{\frac{l\pi v\hbar}{2a} + T\log\left[1 - \exp\left(-\frac{l\pi v\hbar}{aT}\right)\right]\right\}. \tag{A8}$$

Applying Riemann ζ-function regularization ($\sum_{l=1}^{\infty} l = \zeta(-1) = -1/12$) to the first term in Eq. (A8) gives

$$F_{1D}^{(I)} = -\frac{\pi v\hbar}{24a} + T\sum_{l=1}^{\infty}\log\left[1-\exp\left(-\frac{l\pi v\hbar}{aT}\right)\right]. \tag{A9}$$

The summation in the second term evaluates to

$$\sum_{l=1}^{\infty}\log\left[1-\exp\left(-\frac{l\pi v\hbar}{aT}\right)\right] = \frac{\pi v\hbar}{24aT} + \log\left[\eta\left(\frac{\mathrm{i}v\hbar}{2aT}\right)\right], \tag{A10}$$

where $\eta(z)$ is the Dedekind η-function, defined for $\mathrm{Im}[z] > 0$ as

$$\eta(z) = q^{1/24}\prod_{n=1}^{\infty}(1-q^n), \quad (q = \mathrm{e}^{2\mathrm{i}\pi z}). \tag{A11}$$

Substituting Eq. (A10) into Eq. (A9) results in exact cancellation of the a^{-1} terms, yielding the compact expression for the Helmholtz free energy

$$F_{1D}^{(I)} = T\log\left[\eta\left(\frac{\mathrm{i}v\hbar}{2aT}\right)\right]. \tag{A12}$$

References

[1] Casimir H B G 1948 *Proc. Kon. Nederland. Akad. Wetensch.* **51** 793
[2] Milonni P W 1994 *The Quantum Vacuum: An Introduction to Quantum Electrodynamics* (San Diego: Academic Press)
[3] Bordag M, Mohideen U and Mostepanenko V M 2001 *Phys. Rep.* **353** 1–205
[4] Bordag M, Klimchitskaya G L, Mohideen U and Mostepanenko V M 2009 *Advances in the Casimir Effect* (Oxford: Oxford University Press)
[5] Klimchitskaya G L, Mohideen U and Mostepanenko V M 2009 *Rev. Mod. Phys.* **81** 1827
[6] Jaffe R L 2005 *Phys. Rev. D* **72** 021301
[7] Munday J N, Capasso F and Parsegian V A 2009 *Nature* **457** 170
[8] Zhao R, Li L, Yang S, Bao W, Xia Y, Ashby P D, Wang Y and Zhang X 2019 *Science* **364** 984
[9] Zhang Y, Zhang H, Wang X, Wang Y, Liu Y, Li S, Zhang T, Fan C and Zeng C 2024 *Nat. Phys.* **20** 1282
[10] Hertlein C, Helden L, Gambassi A, Dietrich S, Dietrich S and Bechinger C 2008 *Nature* **451** 172
[11] Soyka F, Zvyagolskaya O, Hertlein C, Helden L and Bechinger C 2008 *Phys. Rev. Lett.* **101** 208301
[12] Bonn D, Otwinowski J, Sacanna S, Guo H, Wegdam G and Schall P 2009 *Phys. Rev. Lett.* **103** 156101
[13] Nguyen V D, Faber S, Hu Z, Wegdam G H and Schall P 2013 *Nat. Commun.* **4** 1584
[14] Paladugu S, Callegari A, Tuna Y, Barth L, Dietrich S, Gambassi A and Volpe G 2016 *Nat. Commun.* **7** 11403
[15] Schmidt F, Callegari A, Daddi-Moussa-Ider A, Munkhbat B, Verre R, Shegai T, Käll M, Löwen H, Gambassi A and Volpe G 2023 *Nat. Phys.* **19** 271
[16] Wilson C M, Johansson G, Pourkabirian A, Simoen M, Johansson J R, Duty T, Nori F and Delsing P 2011 *Nature* **479** 376
[17] Lähteenmäki P, Paraoanu G S, Hassel J and Hakonen P J 2013 *Proc. Natl. Acad. Sci. USA* **110** 4234
[18] Felicetti S, Sanz M, Lamata L, Romero G, Johansson G, Delsing P and Solano E 2014 *Phys. Rev. Lett.* **113** 093602
[19] Vezzoli S, Mussot A, Westerberg N, Kudlinski A, Saleh H D, Prain A, Biancalana F, Lantz É and Faccio D 2019 *Commun. Phys.* **2** 84
[20] Chiaverini J, Smullin S J, Geraci A A, Weld D M and Kapitulnik A 2003 *Phys. Rev. Lett.* **90** 151101
[21] Masuda M and Sasaki M 2009 *Phys. Rev. Lett.* **102** 171101
[22] Sushkov A O, Kim W J, Dalvit D A R and Lamoreaux S K 2011 *Phys. Rev. Lett.* **107** 171101
[23] Klimchitskaya G L, Mohideen U and Mostepanenko V M 2012 *Phys. Rev. D* **86** 065025
[24] Wang J, Guan S, Chen K, Wu W, Tian Z, Luo P, Jin A, Yang S, Shao C and Luo J 2016 *Phys. Rev. D* **94** 122005
[25] Sedmik R I P and Pitschmann M 2021 *Universe* **7** 234
[26] Somers D A T, Garrett J L, Palm K J and Munday J N 2018 *Nature* **564** 386
[27] Mostepanenko V M, Trunov N N and Znajek R L 1997 *The Casimir Effect and its Applications* (Oxford: Oxford University Press)
[28] Perivolaropoulos L 2008 *Phys. Rev. D* **77** 107301
[29] Levin M, McCauley A P, Rodriguez A W, Reid M T H and Johnson S G 2010 *Phys. Rev. Lett.* **105** 090403
[30] Zhao R, Zhou J, Koschny T, Economou E N and Soukoulis C M 2009 *Phys. Rev. Lett.* **103** 103602
[31] Song G, Xu J, Zhu C, He P, Yang Y and Zhu S Y 2017 *Phys. Rev. A* **95** 023814
[32] Grushin A G and Cortijo A 2011 *Phys. Rev. Lett.* **106** 020403
[33] Tse W K and MacDonald A H 2012 *Phys. Rev. Lett.* **109** 236806
[34] Rodriguez-Lopez P and Grushin A G 2014 *Phys. Rev. Lett.* **112** 056804
[35] Wilson J H, Allocca A A and Galitski V 2015 *Phys. Rev. B* **91** 235115
[36] Jiang Q D and Wilczek F 2019 *Phys. Rev. B* **99** 125403
[37] Quach J Q 2015 *Phys. Rev. Lett.* **114** 081104
[38] Bellucci S and Saharian A A 2009 *Phys. Rev. D* **80** 105003
[39] Costantino A and Fichet S 2020 *J. High Energy Phys.* **2020** 122
[40] Schecter M and Kamenev A 2014 *Phys. Rev. Lett.* **112** 155301
[41] Nakata K and Suzuki K 2023 *Phys. Rev. Lett.* **130** 096702
[42] Mostepanenko V M 2021 *Universe* **7** 84
[43] Mostepanenko V M, Bezerra V B, Decca R S, Geyer B, Fischbach E, Klimchitskaya G L, Krause D E, López D and Romero C 2006 *J. Phys. A: Math. Gen.* **39** 6589
[44] Mostepanenko V M and Geyer B 2008 *J. Phys. A: Math. Theor.* **41** 164014
[45] Klimchitskaya G L and Geyer B 2008 *J. Phys. A: Math. Theor.* **41** 164032
[46] Lamoreaux S K 2012 *Annu. Rev. Nucl. Part. S.* **62** 37
[47] Hartmann M, Ingold G L and Maia Neto P A 2017 *Phys. Rev. Lett.* **119** 043901
[48] Liu M, Xu J, Klimchitskaya G L, Mostepanenko V M and Mohideen U 2019 *Phys. Rev. B* **100** 081406(R)
[49] Klimchitskaya G L and Mostepanenko V M 2022 *Int. J. Mod. Phys. A* **37** 2241002
[50] Bezerra V B, Klimchitskaya G L, Mostepanenko V M and Romero C 2004 *Phys. Rev. A* **69** 022119
[51] Geyer B, Klimchitskaya G L and Mostepanenko V M 2008 *Eur. Phys. J. C* **57** 823
[52] Nesterenko V V and Pirozhenko I G 1998 *Phys. Rev. D* **57** 1284
[53] Bowers M E and Hagen C R 1998 *Phys. Rev. D* **59** 025007
[54] Cognola G, Elizalde E and Kirsten K 2001 *J. Phys. A: Math. Gen.* **34** 7311
[55] Valuyan M A and Gousheh S S 2010 *Int. J. Mod. Phys. A* **25** 1165
[56] Teo L P 2013 *J. Math. Phys.* **54** 103505
[57] Polchinski J 1998 *String Theory* (Cambridge: Cambridge University Press)
[58] Green M, Schwartz J and Witten E 1987 *Superstring Theory* (Cambridge: Cambridge University Press)
[59] Milton K A, Kalauni P, Parashar P and Li Y 2017 *Phys. Rev. D* **96** 085007
[60] Bordag M 2018 *Phys. Rev. D* **98** 085010
[61] Milton K A, Kalauni P, Parashar P and Li Y 2019 *Phys. Rev. D* **99** 045013
[62] Li Y, Milton K A, Parashar P and Hong L 2021 *Entropy* **23** 214
[63] Sushkov A O, Kim W J, Dalvit D A R and Lamoreaux S K 2011 *Nat. Phys.* **7** 230